



A comprehensive comparison of mixing and mass transfer in shake flasks and their relationship with MAb productivity of CHO cells

Saumel Pérez-Rodríguez¹ · Greta I. Reynoso-Cereceda¹ · Norma A. Valdez-Cruz¹ · Mauricio A. Trujillo-Roldán¹

Received: 21 November 2021 / Accepted: 14 March 2022 / Published online: 26 March 2022
© The Author(s), under exclusive licence to Springer-Verlag GmbH Germany, part of Springer Nature 2022

Abstract

The selection of highly recombinant protein (RP)-productive Chinese hamster ovary (CHO) cell lines is widely carried out in shake flasks. It is assumed that increases in the operating parameters in shake flasks lead to impairments in cell growth and RP production. These effects in cells metabolism are widely associated with high mass transfers and hydrodynamic stress. This study examined the impact of commonly used operational parameters on growth and specific productivity (q_p) of two CHO cell lines differentially secreting a humanized anti-hIL8 monoclonal antibody (mAb) and cultured in 250 ml flasks. The evaluated parameters are filling volume (10, 15, and 20%), shaking frequency (60 and 120 revolutions per minute -rpm-), and orbital diameter (25.4 and 19 mm). The analysis of the oxygen transfer was done in terms of the measured volumetric mass transfer coefficient (k_La) and of the hydrodynamics in terms of power input per unit volume of liquid (P/V), the turbulent eddy length scale measured by the Kolmogorov's microscale of turbulence, the energy dissipation rate, the average shear stress, and the shear rate. Though almost all measured kinetic and stoichiometric parameters remained unchanged, mAb titer included, significant differences were found in maximum cell concentration, 10–45% higher in conditions with lower values of k_La and P/V. Changes in glucose metabolism contributing to q_p were only shown in the higher producer cell line. Non-lethal responses to elevated oxygen transfer and shear stress might be present and must be considered when evaluating CHO cell cultures in shake flasks.

Keywords CHO cells · Specific productivity · Metabolism · Mass transfer · Power input · Shake flasks

Saumel Pérez-Rodríguez and Greta I. Reynoso-Cereceda contributed equally and should be considered co-first authors. This manuscript is dedicated to Dr. Alfredo Torres-Larios an expert on structural and biophysical studies of biological macromolecules.

✉ Mauricio A. Trujillo-Roldán
maurotru@gmail.com

Saumel Pérez-Rodríguez
saumel840217@gmail.com

Greta I. Reynoso-Cereceda
gretareynoso@gmail.com

Norma A. Valdez-Cruz
adri@biomedicas.unam.mx

¹ Unidad de Bioprocessos, Departamento de Biología Molecular y Biotecnología, Instituto de Investigaciones Biomédicas, Universidad Nacional Autónoma de México, Cd. Universitaria, Coyoacán, 04510 Ciudad de México, Mexico

List of symbols

C_L^*	Oxygen concentration at the interfacial saturation
C_L	Oxygen concentration in the liquid bulk
D	Maximum inner flask diameter, m
d_0	Shaking diameter, Mm
d_p	Average cell diameter, m
DOT	Dissolved oxygen tension, % air saturation
IVCC	Integral viable cell concentration, 10^6 cells ml^{-1} day
k_La	Volumetric oxygen transfer coefficient, h^{-1}
Lac/Glc	Lactate/glucose ratio
mAb	Anti-hIL8 monoclonal antibody
n	Shaking frequency, Rpm
Ne'	Modified power number
Ph	Phase number
P/V	Power consumption per unit volume, W m^{-3}
$q_{\text{Ca}^{2+}}$	Specific calcium uptake rate, nmol calcium 10^{-6} cells day^{-1}
q_{Glc}	Specific glucose uptake rate, μMol glucose 10^{-6} cells day^{-1}

q_{Lac}	Specific lactate production rate, $\mu\text{Mol lactate } 10^{-6} \text{ cells day}^{-1}$
q_{Glu}	Specific glutamate production rate, $\mu\text{Mol glutamate } 10^{-6} \text{ cells day}^{-1}$
$q_{\text{NH}_4^+}$	Specific ammonium production rate, $\mu\text{Mol ammonium } 10^{-6} \text{ cells day}^{-1}$
q_p	Specific IgG production rate, $\text{Pcd } 10^{-3}$
Re	Reynolds number
RP	Recombinant protein
t_D	Doubling time, h
ν	Dynamic viscosity, Pa s
V_N	Nominal volume, ml
V_F	Filling volume, % liquid volume/nominal flask volume
V	Filling volume, ml
X_{max}	Maximum cell concentration $10^6 \text{ cells ml}^{-1}$
\mathcal{E}	Energy dissipation rate W kg^{-1}
\mathcal{E}_0	Average energy dissipation rate, W kg^{-1}
ρ	Density, kg m^{-3}
μ	Specific growth rate, h^{-1}
λ	Turbulent eddy length scale, μM
τ	Average shear stress, N m^{-2}
γ	Shear rate, s^{-1}

Introduction

Operational conditions determine the controlled environment experienced by mammalian cells when growing in suspension cultures, affecting process performance and product quality [1, 2]. Mixing aims to maintain cells suspended, promote a uniform distribution of temperature, pH, and nutrients, and ensure gas transfer (oxygen and carbon dioxide) [3, 4]. Conversely, mixing conditions produce hydrodynamic stress capable of potentially damaging mammalian cells [2, 5, 6]. Mixing and aeration in shake flask cultures are accomplished by controlling operational conditions such as the shaking frequency, the flasks nominal volume, the relative filling volume, and the shaking diameter [4, 7, 8]. Previously, it has been demonstrated that changes in those operational conditions can affect cell growth and viability, metabolism, and production in mammalian cells cultures associated with the inefficient gas transfer and the hydrodynamic stress generated [9–13].

In submerged cultures, oxygen transfer results from the aeration delivered at the gas–liquid interphase when flask cultures are shaken. Shaking leads to an increase in oxygen transfer by increasing the mass transfer area. Oxygen transfer rate (OTR) is mathematically defined by Eq. (1) in terms of the volumetric oxygen transfer coefficient ($k_L a$) and the oxygen concentration gradient between the interfacial saturation and the liquid bulk ($C_L^* - C_L$) [3, 14]. The $k_L a$ is an index of the oxygen supply efficiency, and it is proportional to the gas–liquid interfacial area (a).

$$\text{OTR} = k_L a (C_L^* - C_L). \quad (1)$$

Due to the lack of cell wall and their larger size in comparison to microorganisms, animal cells are considered shear sensitive [3, 15–18], being one of the reasons for using low agitation rates (50–200 rpm) in cultures in shaken cylindrical containers [13, 19]. It has been shown that forces of different magnitude would promote cellular lysis or may induce other biological responses like reduced growth, cell death (apoptosis), or different metabolic reactions [5, 6]. Inside submerged cultures, two main fluid mechanical forces are present: shear stress associated with agitation and those related to gas–liquid interface due to sparging [2, 3, 20]. In non-baffled shake flasks, the first one must be considered since bubbles and foam generation are absent, and the flow regime is considered uniform [21–23]. Previously, it has been shown that hybridoma cell growth in shake flask is independent of the specific power input as a shear stress measurement [23]. However, not all animal cells are equally insensitive to a high agitation intensity [3, 11, 24]. The insensitivity of animal cells to hydrodynamic conditions was previously reviewed, covering TB/C3 mouse hybridomas, EBNA cells, HPV cells, and a CHO320 cell line, as well as insect cells [3, 20]. Recent work was published evaluating various orbitally shaken single-use cultivation systems (500 ml Erlenmeyer shake flask, the cylindrical TubeSpin bioreactor, and the alternately designed Optimum Growth flask) and presenting, as a result, a design space that allows optimal growth of a CHO cell line in submerged cultures [13]. However, the authors do not present lower volume shake flasks nor CHO cell lines producing recombinant proteins (RPs).

Here, we analyzed the culture performance of two recombinant CHO cell lines producing a humanized monoclonal antibody (mAb) with a 26-fold difference in their specific productivity (q_p) [25] in terms of growth, cell viability, substrate consumption, metabolite, and ions accumulation and RP production, in suspension cell cultures growing in 250 ml Corning flasks shaken at different conditions ($n = 60/120 \text{ rpm}$; $d_o = 25.4/19.1 \text{ mm}$) and filling volume (10, 15 and 20%). These comparisons were made concerning the initial $k_L a$, and volumetric power input (P/V) applied to submerged cultures.

Materials and methods

Cell lines and culture conditions

Cell lines CHO DP-12 clone #1933 CRL-12444 and clone #1934 CRL-12445 [26], which secrete a humanized anti-hIL8 monoclonal antibody (mAb), were acquired from the American Type Culture Collection (ATCC). Cells were

cultured in CDM4CHO medium (Hyclone, Logan, UT, USA) supplemented with 6 mM stable glutamine (Alanyl-glutamine dipeptide, Biowest LLC, Kansas City, MO, USA), 0.002 mg/ml Humulin N (Eli Lilly, Indianapolis, IN, USA) and 200 nM methotrexate (Pfizer, New York, NY, USA), at 37 °C in a 5% CO₂ atmosphere in a humidified incubator.

Cells from cultures with viability higher than 95% were seeded at 0.50×10^6 cells/ml in 250 ml Corning Erlenmeyer flasks (Cat. 431144, Corning, Glendale, AZ, USA), at 10 (25 ml), 15 (37.5 ml) and 20 (50 ml) % filled volumes, at 60 rpm (Cat. 7644-10115 Bellco Glass Inc., Vineland, N.J., USA, $d_0=25.4$ mm) and 120 rpm (Thermolyne, Big Bill, USA, $d_0=19.1$ mm). Cell concentration and viability were measured every 24 h by counting in a Neubauer chamber using the trypan blue dye exclusion method [27]. Culture time at which viability was above 90% was inferred from a 100 segments viability cubic spline curve generated by GraphPad Prism Software v5.01 (GraphPad Software, San Diego, CA, USA).

Quantification of metabolites, ions, and pH

The concentration of glucose, lactate, glutamine, glutamate, ammonium, sodium, potassium, and calcium in culture supernatants was measured every 24 h using BioProfile FLEX2 Automated Cell Culture Analyzer (Nova Biomedical, Waltham, MA, USA). Glucose concentration was also measured in the A15 automatized analyzer (Biosystems, Barcelona, Spain). Specific consumption or production rates were calculated during the exponential growth phase as the ratio between metabolite concentration and the integral viable cell concentration (IVCC), obtained as Area Under Curve using GraphPad Prism Software v5.01 (GraphPad Software, San Diego, CA, USA).

Quantification of specific productivity (q_p)

Anti-hIL8 mAb concentration was measured every 24 h using Human IgG ELISA Quantitation Set (E80-104, Bethyl Laboratories, Inc., Montgomery, TX, USA), according to manufacturer's protocol. SigmaFast OPD substrate (Sigma-Aldrich, Merck KGaA, Darmstadt, Germany) was prepared according to the manufacturer's recommendations and incubated at room temperature for 15 min. The enzymatic reaction was stopped by adding 10% (v/v) HCl, and absorbance was recorded at 490 nm. q_p values were calculated during the exponential growth phase as the ratio between product concentration and IVCC.

Volumetric mass transfer coefficient ($k_L a$)

A 250 ml polycarbonate Corning Erlenmeyer flask was filled with 25, 37.5, or 50 ml of water and placed in an incubator

with controlled conditions at 37 °C and 5% CO₂ (NuAire, USA). Shaking frequency was set at 120 rpm with 19 mm shaking diameter (0.75 in) (Thermolyne, Big Bill, USA); or at 60 rpm with 25.4 mm (1 in) shaking diameter (Cat. 7644-10115 Bellco Glass Inc., Vineland, N.J., USA). The measurements of $k_L a$ were performed as described elsewhere [28] but subjected to the CO₂ atmosphere. Briefly, measurements were obtained using the gassing-out method: oxygen was removed from water by adding Na₂SO₃ and CoCl₂ as catalysts to achieve final concentrations below 6×10^{-3} and 5×10^{-7} mol L⁻¹, respectively. Orbital shaker was started once oxygen-free water was assured, and the dissolved oxygen tension (DOT) was recorded online with an oxygen optical meter Fibox3 using a PSt3 sensor (PreSens, Regensburg, Germany). The sensor patch was attached at the bottom of the Corning flask, and the optic fiber was fixed in the shaker placed inside the CO₂ incubator. The PSt3 sensors have a response time (measure at 63% of the response) near 14 s, which allows for the measurement of $k_L a$ up to 250 h⁻¹ using the van't Riet criterion [13, 29].

The $k_L a$ of four independent measurements per condition was obtained as the linear slope from a plot of the logarithmic expression against time Eq. (2) [5, 14, 27], where $C_L^* = 100\%$ saturated air, C_{L1} and C_{L2} are the DOT recorded at time points t_1 and t_2 , respectively.

$$\ln\left(\frac{C_L^* - C_{L2}}{C_L^* - C_{L1}}\right) = -k_L a \times (t_2 - t_1) \quad (2)$$

For comparison purposes, $k_L a$ values were also calculated using the empirical correlation reported by Klöckner and Büchs [8] (Eq. 3).

$$k_L a = 0.0003212d^{1.92}n^{1.16}d_0^{0.38}V^{-0.83}, \quad (3)$$

where d is the maximum inner flask diameter ($d=0.08$ m), n is the shaking frequency (s⁻¹), d_0 is the shaking diameter (m), and V is the filling volume (m³).

Calculation of power input (P/V), flow field and hydrodynamic parameters

P/V was calculated as a function of the operational conditions (Eq. 4) and the Reynolds number (Eq. 5) using the correlation proposed by Büchs et al. [21, 30], as follows:

$$\frac{P}{V} = \frac{C\rho n^3 d^4}{Re^{0.2}V^{2/3}} \quad (4)$$

$$Re = \frac{\rho n d^2}{\mu}, \quad (5)$$

where P/V is the power consumption per unit volume (W m^{-3}), C is a non-linear fitting constant ($C=1.94$), n is the shaking frequency (s^{-1}), d is the maximum inner flask diameter ($d=0.08$ m), and V is the liquid volume (m^3). The physicochemical constants ρ (kg m^{-3}) and ν (Pa s) are the density and the dynamic viscosity of water at 37 °C since the cell/medium suspension is water-like [20].

Cell stress in the flow field inside shake flask cultures depends on cell size relative to an appropriate turbulent eddy length scale λ (m), measured by the Kolmogorov's microscale of turbulence, which can be directly related to the energy dissipation rate (\mathcal{E}) according to Eq. (6) [21, 23, 30, 31].

$$\lambda = \left(\frac{\mu}{\rho} \right)^{3/4} \varepsilon_0^{-1/4}. \quad (6)$$

The average energy dissipation rate \mathcal{E}_0 (W kg^{-1}) for non-baffled flasks is obtained from Eqs. (7) and (8) in function of the Reynolds number (Eq. 5) [21, 30, 32].

$$\varepsilon_0 = \frac{Ne'm^3 d^4}{V^{2/3}} \quad (7)$$

$$\varepsilon_0 = \frac{Ne'm^3 d^4}{V^{2/3}}. \quad (8)$$

Ne' is the modified power number for non-baffled flasks, influenced by the Reynolds number and the geometrical dimensions. Equation (8) resulted from the fitted model proposed by Büchs et al. [21, 30], for liquids with water-like viscosity and has a laminar (Re^{-1}), a transition ($Re^{-0.6}$), and a turbulent term ($Re^{-0.2}$).

For calculation of the average shear stress τ (N m^{-2}) and the shear rate γ (s^{-1}), it is necessary to consider the average cell diameter d_p (m), as indicated in Eqs. (9) and (10) [31].

$$\tau = 0.0676 \left(\frac{d_p}{\lambda} \right)^2 (\rho \nu \varepsilon_0)^{1/2} \quad (9)$$

$$\gamma = \frac{\tau}{\nu}. \quad (10)$$

Statistical analysis

All cultures were carried out three times. One-way ANOVA followed by Tukey's Multiple Comparison Test was used when needed to estimate statistical significance in the culture parameters. Pearson correlation coefficient was determined for correlation analyses. A threshold significance level of 0.05 was applied for all analyses in GraphPad Prism v5.01. LOESS regression models were fitted to the experimental kinetic and stoichiometric parameters for CRL-12444 and

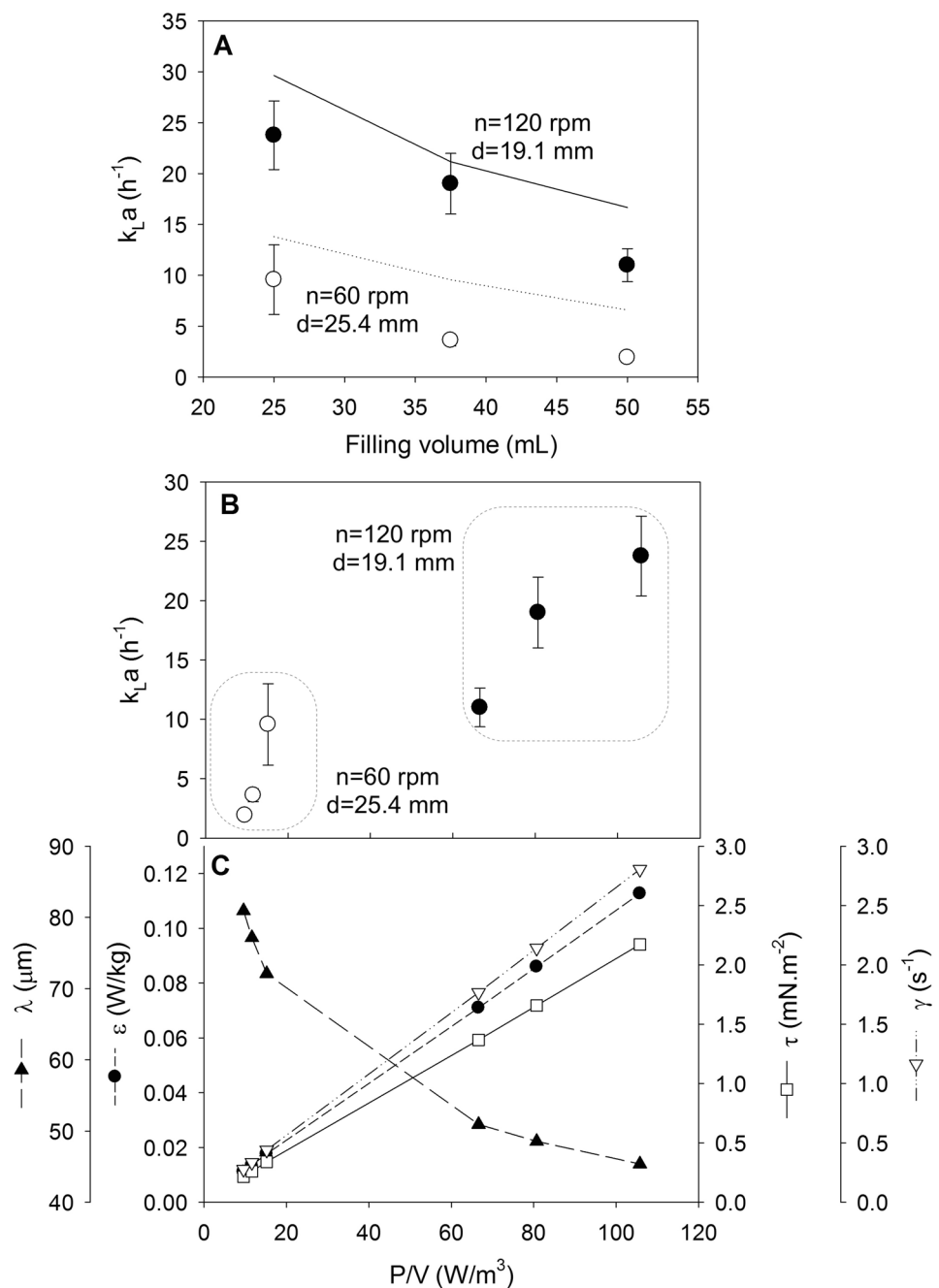
CRL-12445 cells in R language to predict μ ($\alpha=0.80$), t_D ($\alpha=0.70$), X_{max} ($\alpha=0.80$), $IVCC$ ($\alpha=0.85$), q_P ($\alpha=0.75$), q_{Glc} ($\alpha=0.85$), Lac/Glc ratio ($\alpha=0.87$) and $q_{\text{Ca}^{2+}}$ ($\alpha=0.80$) values. Local polynomial regression fitting of second degree used experimental P/V and k_{LA} as numerical predictors.

Results

The k_{LA} values were measured at the different shaking rates and filling volumes chosen for culturing CHO cells (Fig. 1A). It has been previously shown that k_{LA} increases with shaking frequency, flask size, and shaking diameter [4, 7, 8]. Our results show how by maintaining the same flask diameter, the shaking frequency of 120 rpm promotes higher k_{LA} values compared with 60 rpm, even when the shaking diameter was lower (19.1 vs. 25.4 mm), which can be explained by the higher P/V values delivered at 120 rpm (Fig. 1B). A positive correlation between P/V and k_{LA} experimental values was found in our study, explaining why P/V -derived results might mirror those from k_{LA} (Pearson $r=0.94$), although there is a sudden change between the two incubators used indeed due to the rotational diameter (19.1 vs. 25.4 mm; Fig. 1B). We can also observe that k_{LA} is greater at the lower filling volumes (Table 1) as it is expected due to the higher interfacial area–volume ratio [28]. Figure 1A also shows the theoretical values of k_{LA} at the different operational conditions according to an empirical model found in the literature (Eq. 3) [8], which were higher than the experimental values. Figure 1C shows the linear correlation between P/V , the average energy dissipation rate (\mathcal{E}_0), the average shear stress (τ), and the shear rate (γ), as Table 1 resumes. Thus, when analyzing the effect of P/V on recombinant CHO cells cultures, similar conclusions can be obtained with these hydrodynamic factors (\mathcal{E}_0 , τ , and γ). However, there is a non-linear inverse correlation between P/V and the size of the turbulent eddy length scale measured by Kolmogorov's microscale of turbulence (λ) (Fig. 1C). This Kolmogorov's microscale of turbulence is considered an index of the potential cell damage. Whenever the cellular size is minor than λ , the hydrodynamic stress is not assumed as harmful [3, 20, 24, 31]. The typical cellular size of CHO cells is between 15 and 18 μm [33], so according to Kolmogorov's theory, λ values estimated here between 45.4 and 80.9 μm (Table 1) are unlikely to cause cellular damage [20].

Thus, once the culture system was characterized in mass transfer and hydrodynamic stress, the effects of agitation rate and filling volume of the shake flasks on growth kinetics of two CHO cell populations secreting a humanized anti-hIL8 mAb were assessed (Fig. 2). The clone CRL-12444 remains viable ($>90\%$) at least 3 days more than

Fig. 1 **A** k_La values of 250 ml Corning flasks shaken at 120 rpm (filled dots) and 60 rpm (empty dots) maintained at 37 °C, 5% CO₂, and varying the relative filling volume at 10, 15, and 20%. Means and standard deviations of four independent measurements are shown. Theoretical k_La values were calculated according to the model published by Klöckner and Büchs (2012) and are represented as a dotted line (120 rpm, $d_0=19$ mm) and a straight line (60 rpm, $d_0=25.4$ mm). **B** Relationship between volumetric power (P/V) and k_La for the 250 ml Corning flasks shaken at 120 rpm (dots) and 60 rpm (triangles) at three filling volumes. **C** Relationship of P/V , the turbulent eddy length scale measured by the Kolmogorov's microscale of turbulence (λ), the energy dissipation rate (\mathcal{E}), the average shear stress (τ) and the shear rate (γ) as published in Table 1



clone CRL-12445. In addition, the cultures carried at 60 rpm present up to 10–45% more maximum cell concentration (X_{max}) than those grown at 120 rpm (in almost all filling volumes evaluated). Sublethal effects could explain this due to elevated oxygen transfer rate or shear stress [34]. Kinetics of glucose, lactate, glutamine, glutamate, and ammonium concentration, and pH in supernatants in supernatants of CHO cell cultures are shown in Fig. S1. It is worth noting that the cultures carried at 120 rpm present up to 20.0–80.6% more glutamine in the supernatant than those grown at 60 rpm (in all filling volumes evaluated)

when using the clone CRL-12444. Still, when using the clone CRL-12445, these differences in glutamine production were found only on the second day of culture (Fig. S1). Whether these glutamine concentrations reflect its specific consumption rate could not be known, because the biochemistry analyzer cannot quantify this amino acid as a dipeptide form. As has been reported in other cell lines, low oxygen conditions can promote glutamine uptake by increasing glutamine transporters, switching the fate of glutamine from the oxidative pathway into the reductive carboxylation pathway [35]. Moreover, kinetic of sodium,

Table 1 Operational conditions used with the measured volumetric oxygen transfer coefficient, volumetric power input, flow field, and hydrodynamic parameters estimated for each experimental shaking condition of the 250 ml shake Corning flasks cell suspended cultures

Shaking frequency (rpm)	Shaking diameter (mm)	Volume (ml)	Relative filling volume (%)	k_La (h^{-1})	Re (–)	P/V (W m^{-3})	\mathcal{E}_0^a (W kg^{-1})	λ^a (μm)	τ^a (mN.m^{-2})	γ^a (s^{-1})
120	19.0	25.0	10	23.76	16,375	105.7	0.113	45.4	2.17	2.81
		37.5	15	19.01		80.7	0.086	48.5	1.66	2.14
		50.0	20	11.00		66.6	0.071	50.9	1.37	1.77
60	25.4	25.0	10	9.57	8188	15.2	0.018	72.1	0.34	0.44
		37.5	15	3.61		11.6	0.013	77.1	0.26	0.34
		50.0	20	1.92		9.6	0.011	80.9	0.21	0.28

^aCalculations for the hydrodynamic parameters are based on the turbulent regime flow ($\text{Re} > 60,000$). However, both conditions are not fulfilled (Büchs et al. 2000 [21]; Peter et al. 2006 [32]). Therefore, results are presented as an approximation and must be carefully interpreted

potassium, and calcium concentrations on culture media are shown in Fig. S2, and when comparing 60–120 rpm, no significant differences were found. However, both cell lines tend to consume more calcium at 120 rpm than at 60 rpm in flasks with 20% filled volume (Fig. S2).

Kinetic and stoichiometric parameters were calculated for each experimental shaking condition of the suspension cultures in Corning flasks (Table S1) and plotted against the k_La (Fig. 3). The clone CRL-12444 statistically presented a higher maximum cell concentration at lower values of k_La (that corresponds to 60 rpm, $d_0=25.4$ mm, Fig. 3). In contrast, a statistical significance for X_{max} was only reached between 9.57 and 11.00 h^{-1} in the case of CRL-12445 cells. The rest of the parameters measured in CRL-1244 cells did not change in any condition (Fig. 3). In the case of CRL-12445, a higher q_p was obtained at the mid-value of k_La (11.0 h^{-1} , Fig. 3L), but without effect on the final concentration of the mAb (Fig. 3F). This is surely associated with the reduction in the IVCC in the same value of k_La (Fig. 3E). For these higher producer cells (CRL-12445) in this mid k_La value, it was recorded an increased glucose consumption (q_{Glc}) (Fig. 3G) without changes in lactate production (q_{Lac}) (Fig. 3H), which translated into a lower Lac/Glc ratio (Fig. 3I).

Comparing the kinetic and stoichiometric parameters based on P/V, the clone CRL-12444 statistically presented a higher X_{max} at lower values of P/V (that corresponds to 60 rpm, $d_0=25.4$ mm, Fig. 4). Like k_La , CRL-12445 presented a q_p at the mid-value of P/V (66.6 W m^{-3} , Fig. 4L) without effect on the final concentration of the mAb (Fig. 4F). It is worth noting that in both clones, the final concentration of the mAb was not affected as an effect of k_La or P/V (Figs. 3F, 4F). Though without statistical significance, a tendency to a higher growth rate and shorter doubling time was observed in both cell lines at lower k_La and P/V values. The same kinetic and stoichiometric parameters were plotted as a function of the filling volume and shaking rates in both clones in Fig. S3.

Trends in μ , t_D and calcium consumption for CRL-12444 cells, and the statistical differences in X_{max} , IVCC, q_p , q_{Glc} , and Lac/Glc ratio for CRL-12445 cells were fully reflected on the predicted behavior of these parameters in correspondence with k_La and P/V values by regression models (Fig. 5).

Discussion

Mammalian cells have a slow growth related to a low oxygen uptake rate compared to yeast or bacterial cultures [2, 3]. The k_La coefficient is not an index of cellular oxygen consumption, but it can be indirectly related. It has been reported that low values of OTR around $0.5\text{--}8 \times 10^{-10}$ $\text{mmol L}^{-1} \text{h}^{-1}$ are enough to supply the oxygen demand of a 10^7 cells ml^{-1} culture [36, 37]. Particularly, for CHO cells in suspension cultures, k_La typical values are usually in the range of 1 to 60 h^{-1} (Fig. 6, Table S2). For example, k_La values between 3 and 50 h^{-1} should satisfy oxygen demand for a 10^7 cells ml^{-1} culture [20, 37]. Here, we measured k_La values in water between 1.9 and 23.8 h^{-1} (Fig. 1A, B, Table 1), so it is expected that flasks shaken at 60 rpm, even the higher shaking diameter (25.4 mm), and the higher filling volumes are potentially more likely to promote oxygen restricted cultures, even more so when high cell densities are reached [13, 38]. Measured values of k_La at the different operational conditions were lower compared with the empirical model found in the literature (Eq. 3) [8]. As expected, theoretical values tend to be higher than the experimental k_La values since the Corning flasks are made of hydrophobic polycarbonate material. In contrast, the model presented was experimentally validated for hydrophilic glass flasks. Flask walls nature plays an essential role in oxygen transfer. It has been shown a film formation of liquid at flask walls that significantly increases gas–liquid interfacial area associated with the centrifugal movement of the fluid during the orbital shaking. The formation of this thin film is abolished in flask walls of hydrophobic nature [7, 39].

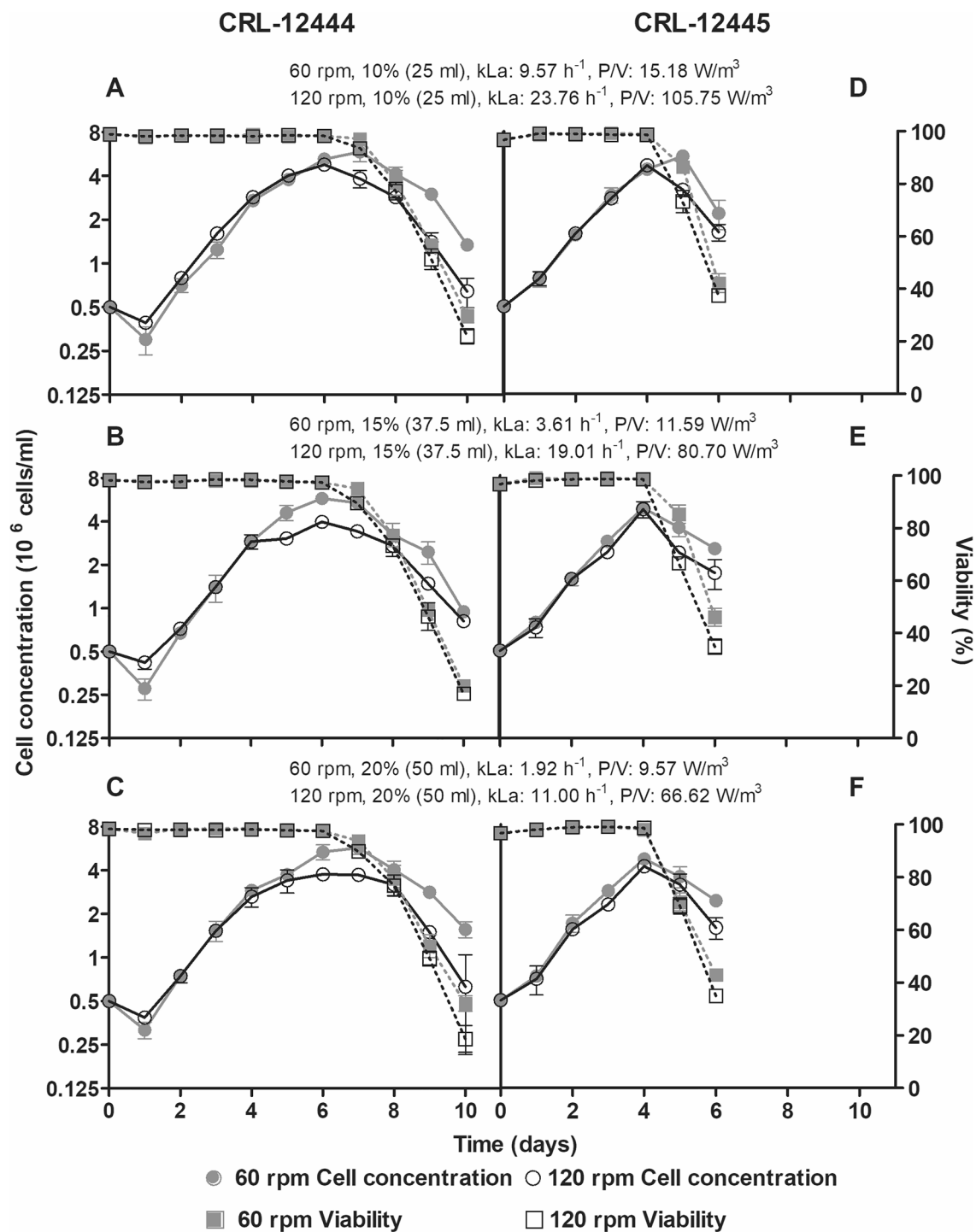


Fig. 2 Effects of agitation speed on growth kinetics of Chinese hamster ovary cells producing a monoclonal antibody. CRL-12444 (A–C) and CRL-12445 (D–F) cells were seeded at 0.5×10^6 cells/ml in 250 ml Erlenmeyer flasks at 10 (A, D), 15 (B, E) and 20% (C, F) filled volumes, at 60 (closed symbols) and 120 (open symbols) rpm.

Viable cell concentration (circles in continuous lines) and viability (squares in dotted lines) of cultures were determined over time by the trypan blue dye exclusion method in a Neubauer chamber. Error bars represent the standard deviation of three biological replicates

Furthermore, the oxygen transfer experimented by CHO cells is expected to be even lower due to solutes in culture media that negatively affects oxygen solubility (C_L) and

the global oxygen transfer coefficient (k_L) [40, 41]. Moreover, since the controlled atmosphere inside the incubator has lower oxygen partial pressure than air, due to the CO_2

Fig. 3 Effects of $k_L a$ on kinetic and stoichiometric parameters of CRL-12444 (closed dots) and CRL-12445 (open dots) CHO cells producing a monoclonal antibody. Specific growth rate (μ , **A**), doubling time (t_d , **B**), maximum cell concentration (X_{max} , **C**), time at which viability was above 90% (**D**), integral of viable cell density (IVCC, **E**), monoclonal antibody concentration (**F**) are presented. Moreover, specific consumption of glucose (**G**), specific production of lactate (**H**), glutamate (**J**), ammonium (**K**), and monoclonal antibody (**L**) were presented, as well as the ratio of glucose and lactate specific rates (**I**). Error bars represent the standard deviation of three biological replicates

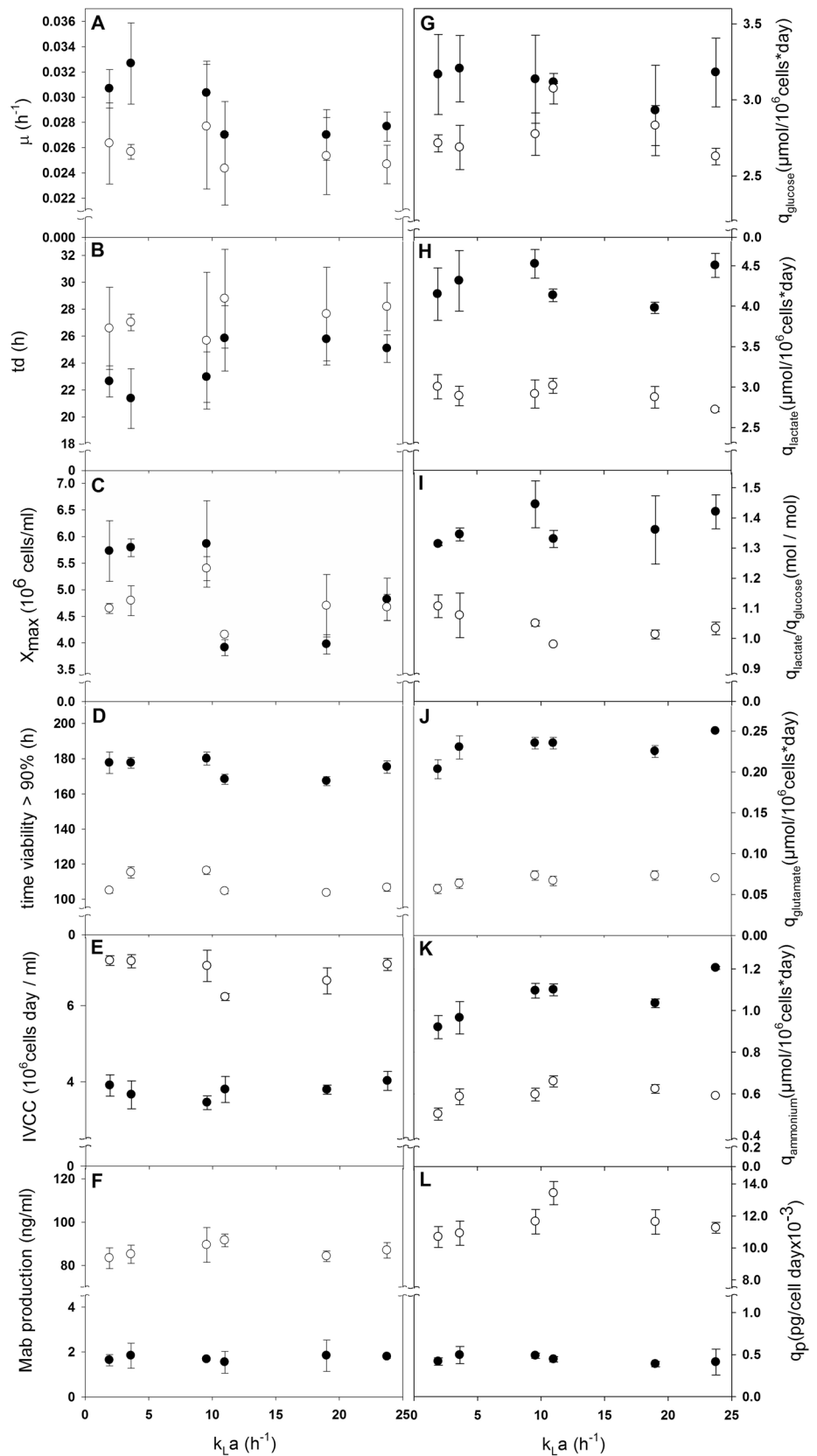
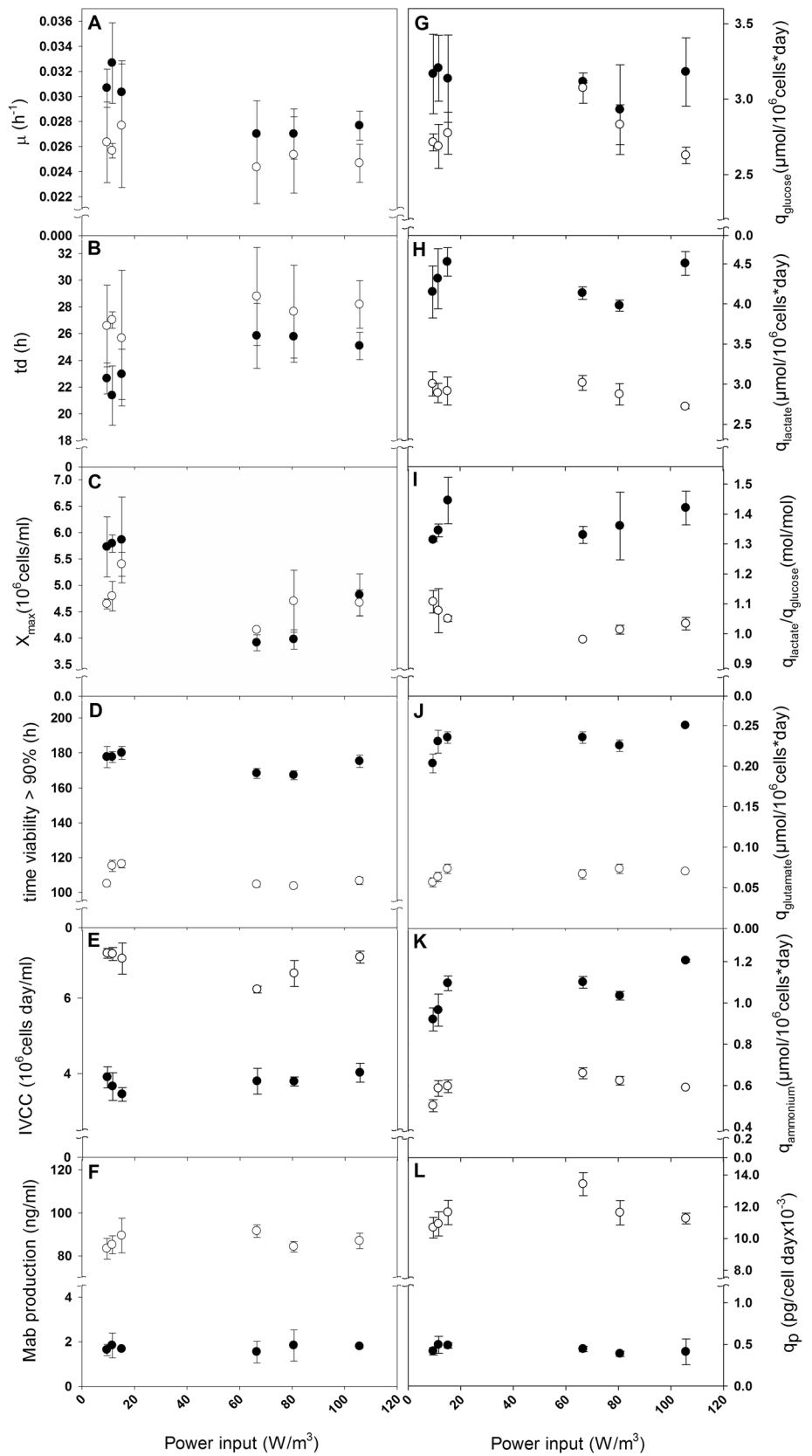


Fig. 4 Effects of volumetric power input (P/V) on kinetic and stoichiometric parameters of CRL-12444 (closed dots) and CRL-12445 (open dots) CHO cells producing a monoclonal antibody. Specific growth rate (μ , **A**), doubling time (t_d , **B**), maximum cell concentration (X_{max} , **C**), time at which viability was above 90% (**D**), integral of viable cell density (IVCC, **E**), monoclonal antibody concentration (**F**) are presented. Moreover, specific consumption of glucose (**G**), specific production of lactate (**H**), glutamate (**J**), ammonium (**K**), and monoclonal antibody (**L**) were presented, as well as the ratio of glucose and lactate specific rates (**I**). Error bars represent the standard deviation of three biological replicates



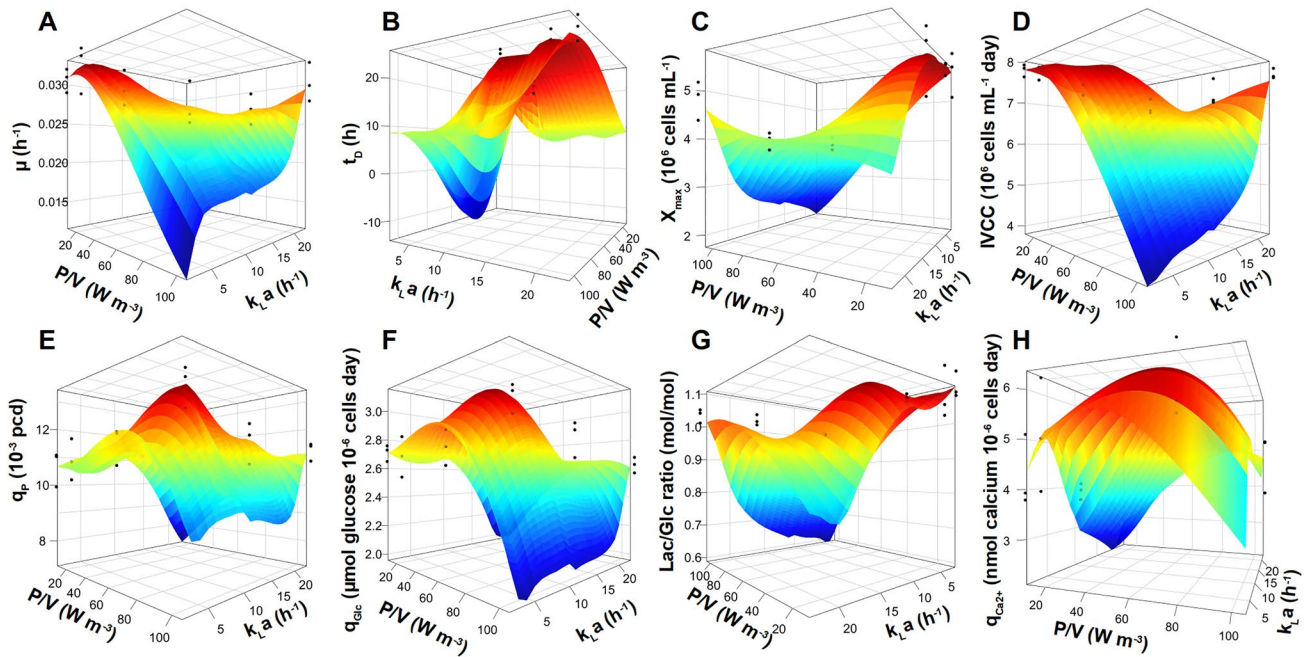


Fig. 5 LOESS regression models of kinetic and stoichiometric parameters of Chinese hamster ovary cells producing an anti-hIL8 monoclonal antibody under different P/V and k_La conditions. A polynomial surface of the second degree was fitted to experimental data

using P/V and k_La as numerical predictors for μ (A), t_D (B), X_{\max} (C), and IVCC (D) from CRL-12444 cells, and q_P (E), q_{Glc} (F), Lac/Glc ratio (G), and $q_{\text{Ca}^{2+}}$ (H) from CRL-12445. The predicted z-axis ranges from high (red) to low (blue) values

atmosphere, the oxygen available is expected to be lower than that reported at similar conditions with orbitally shaken flasks [42]. Low oxygen transfer rates, related to lower agitation rates, could lead to variations of the culture pH [3, 42]. Also, CO_2 produced could not be completely stripped out of the media, promoting physiologically dangerous levels of pCO_2 [3, 42]. Even with all these problems, in our case, the production of a mAb being the main objective, we do not see important effects of the filling volume, diameter, and stirring speed, all associated with k_La , on the product titer (Fig. 3). Though final product titer and quality

are two of the most critical parameters for a successful bioprocess, the changes in q_P and metabolism experimented with by cells over time could give crucial clues for process improvement. In this line, intermediate k_La (11 h^{-1}) and P/V (66.62 W m^{-3}) values impact on productivity and metabolism of the higher producer cells (CRL-12445). The positive correlation between k_La and P/V values in shake flasks and most orbitally shaken single-use bioreactors derives from the impossibility of separating these variables. It is reflected in previous reports even in different culture conditions (Pearson coefficient $r=0.62$, Fig. 6). CRL12445 cells at these mid values increase glucose consumption without changing lactate production, resulting in a lower Lac/Glc ratio. This higher efficiency in glucose conversion could contribute to the higher q_P exhibited by CHO cells [43]. Thus, these intermediate ranges of k_La and P/V could be harnessed during bioprocesses to shift CHO cells toward a more efficient carbon metabolism and circumvent in this way the genetic engineering [44] or the challenging task of maintaining low nutrient levels [45] required for this purpose.

The volumetric power input (equivalent to the mean specific energy input rate) is dissipated in the bioreactor or shake flask through a series of eddy cascades, which eventually converts all mechanical energy into heat. Energy dissipation is the driving force for mixing and the cause of the hydrodynamic stress on the cells [16, 17]. Since mammalian cells have low oxygen demand, the rate of energy input is

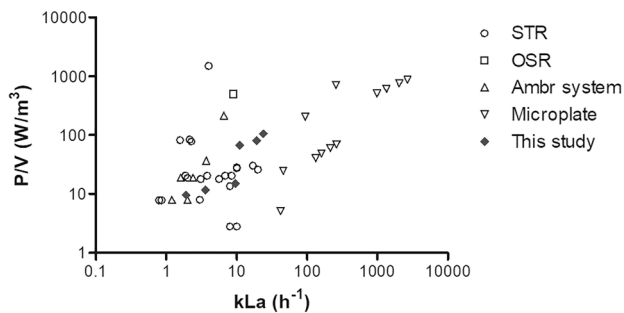


Fig. 6 Relation of P/V and k_La values of CHO cell cultures obtained from the literature. Data were taken from Table S2. Stirred tank bioreactors (STR, circles); Orbitally shaken reactors (OSR, squares); Ambr™ systems (triangles); microplates (inverted triangles) and shake flasks in this work (filled diamonds)

also low, typically between 1 and 10 W m^{-3} , allowing efficient operation in shake flasks [2, 3]. Using the correlation proposed by Büchs et al. [21, 29] (Eq. 4), we estimated the power input values in function of the shaking operational conditions (Fig. 1, Table 1). Results obtained are between 9.6 and 15.2 W m^{-3} ($n = 60 \text{ rpm}$) and 66.6 – 105.7 W m^{-3} ($n = 120 \text{ rpm}$), which exceed the mean power input requirements for mammalian cell suspension cultures. Moreover, the values calculated agree with those previously reported [21, 30]. Compared with the $k_L a$ values measured for the Corning flasks, the hydrophobic nature of the flask walls has no relevant impact on the power consumption [21, 30].

To determine how significant the mixing shear stress is, we also calculated the turbulent eddy length scale (λ), the average energy dissipation rate (\mathcal{E}_0), the average shear stress (τ) and the shear rate (γ) (Eqs. 6–10). Those models for the hydrodynamic parameters are based on the turbulent regime flow ($Re > 60,000$). However, this condition is not fulfilled [32], but there is an advantage that the ratio of maximum and average energy dissipation rates is almost 1.0 [32]. Therefore, results in Table 1 corresponding to the hydrodynamic parameters for shaken flasks are only presented as an approximation and must be carefully interpreted.

At 120 rpm, the average energy dissipation rate (\mathcal{E}_0) calculated were 0.071 – $0.113 \text{ (W kg}^{-1}\text{)}$, while the average shear stress and the shear rate were 1.37 – 2.17 mN m^{-2} and 1.77 – 2.81 s^{-1} , respectively (Table 1), considering an average cell diameter of $15 \mu\text{m}$ [33]. Those hydrodynamic parameters had low values and were even lower when calculated at the shaking frequency of 60 rpm (Fig. 1C, Table 1). Animal cells are insensitive to low shear stress, and no effects are reported associated with energy dissipation rates (\mathcal{E}) lower than 100 W kg^{-1} [6, 17]. Animal cells death associated with high shear stress occurs typically with \mathcal{E} values between 10^7 and 10^8 W kg^{-1} . However, lethal effects have also been reported at \mathcal{E} values near 10^3 W kg^{-1} [6, 17]. This literature information may help to explain why we do not find significant differences in mAb final concentration, besides some sub-lethal effects as a higher specific growth rate, a shorter doubling time, and a higher maximum cell concentration were found at lower values of P/V (mainly in the clone CRL-12444, Fig. 4). A few studies have published sub-lethal effects elicited by hydrodynamic forces, like slow growth, altered glucose metabolism, reduced productivity, and RP glycosylation profile change produced by CHO cells [15, 17, 46]; at \mathcal{E} values between 10^3 and 10^5 W kg^{-1} , which correspond to shear stresses on the order of 1 – 10 N m^{-2} [6, 17]. Moreover, no effect on cell viability or antibody-produced quality was found in three CHO cell lines cultivated in bioreactors with \mathcal{E} values of 0.01 – 0.02 and 1 W kg^{-1} [3, 20].

Conclusions

Here, we show that hydrodynamic conditions inside non-baffled shake flasks are unlikely to elicit cellular damage with the previous data. Though these responses are line-specific, there is still the possibility of some response to the higher energy dissipation experienced by cells at 120 rpm, like the decrease in the maximum cell concentration, which, along with metabolic impact, are expected to be non-lethal responses. The widely used conditions for suspended CHO cell cultures in shake flasks presented in this work are suitable. However, at the lower shaking frequency and higher filling volumes, the risk of getting mass transfer limited is present, whereas at the higher shaking frequency of 120 rpm and the lower non-lethal responses to shear stress may be present.

Supplementary Information The online version contains supplementary material available at <https://doi.org/10.1007/s00449-022-02722-y>.

Acknowledgements Greta I. Reynoso-Cereceda is a doctoral student from Programa de Doctorado en Ciencias Biomédicas, Universidad Nacional Autónoma de México (UNAM) and received the fellowship number 478675, from “Consejo Nacional de Ciencia y Tecnología” CONACYT. We want to extend our gratitude to Sartorius de México, S.A. de C.V. and Biosystems S.A. de C.V. Also, we thank to Nova Biomedicals for providing access to BioProfile FLEX2 Automated Cell Culture Analyzer.

Author contributions Conceptualization: SP-R, GIR-C, NAV-C, and MAT-R; methodology: SP-R and GIR-C; formal analysis and investigation: SP-R, GIR-C, NAV-C, and MAT-R; writing—original draft preparation: SP-R and GIR-C; writing—review and editing: SP-R, GIR-C, NAV-C, and MAT-R; funding acquisition: NAV-C and MAT-R; resources: NAV-C and MAT-R.

Funding This work was supported by “Programa de Apoyo a Proyectos de Investigación e Innovación Tecnológica, Universidad Nacional Autónoma de México” (PAPIIT-UNAM IN210419, IN210822, IN211422, IV201220). Funding sources had no role in study design, data collection and analysis, decision to publish, or preparation of the manuscript.

Data availability The datasets generated during and analyzed during the current study are available from the corresponding author on reasonable request.

Declarations

Conflict of interest Authors declare that they have no conflict of interest.

References

1. Trummer E, Fauland K, Seidinger S, Schriebl K, Lattenmayer C, Kunert R, Vorauer-Uhl K, Weik R, Borth N, Katinger H, Müller D (2006) Process parameter shifting: Part I. Effect of DOT, pH,

- and temperature on the performance of Epo-Fc expressing CHO cells cultivated in controlled batch bioreactors. *Biotechnol Bioeng* 94(6):1033–1044. <https://doi.org/10.1002/bit.21013>
2. Zhang H, Wang W, Quan C, Fan S (2010) Engineering considerations for process development in mammalian cell cultivation. *Curr Pharm Biotechnol* 11(1):103–112. <https://doi.org/10.2174/138920110790725320>
 3. Nienow AW (2015) Mass transfer and mixing across the scales in animal cell culture. In: Al-Rubeai M (ed) *Animal cell culture*. Springer, Dublin, pp 137–167. https://doi.org/10.1007/978-3-319-10320-4_5
 4. Sundaramurthy S (2009) Mixing in shake flask bioreactor. *Encyclopedia of industrial biotechnology*. In: Flickinger MC (ed) *Bioprocess, bioseparation, and cell technology*. John Wiley & Sons Inc., pp 1–17. <https://doi.org/10.1002/9780470054581.eib662>
 5. Czermak P, Pörtner R, Brix A (2009) Special engineering aspects. In: Eibl R, Eibl D, Pörtner R, Catapano G, Czermak P (eds) *Cell and tissue reaction engineering*. Springer, Berlin. https://doi.org/10.1007/978-3-540-68182-3_4
 6. Chalmers JJ, Ma N (2015) Hydrodynamic damage to animal cells. In: Al-Rubeai M (ed) *Animal cell culture*. Springer, Dublin, pp 169–183. https://doi.org/10.1007/978-3-319-10320-4_6
 7. Maier U, Büchs J (2001) Characterization of the gas-liquid mass transfer in shaking bioreactors. *Biochem Eng J* 7(2):99–106. [https://doi.org/10.1016/S1369-703X\(00\)00107-8](https://doi.org/10.1016/S1369-703X(00)00107-8)
 8. Klöckner W, Büchs J (2012) Advances in shaking technologies. *Trends Biotechnol* 30(6):307–314. <https://doi.org/10.1016/j.tibtech.2012.03.001>
 9. Micheletti M, Barrett T, Doig SD, Baganz F, Levy MS, Woodley JM, Lye GJ (2006) Fluid mixing in shaken bioreactors: Implications for scale-up predictions from microlitre-scale microbial and mammalian cell cultures. *Chem Eng Sci* 61(9):2939–2949. <https://doi.org/10.1016/j.ces.2005.11.028>
 10. Abidin SZ, Anuar N (2011) Comparison of the production of recombinant protein in suspension culture of CHO cells in spinner flask and shake flask system. *IJUM Eng J* 12(4):43–49. <https://doi.org/10.31436/ijumej.v12i4.180>
 11. Platas OB, Sandig V, Pörtner R, Zeng AP (2013) Evaluation of process parameters in shake flasks for mammalian cell culture. *BMC Proc (BioMed Central)* 7(6):17. <https://doi.org/10.1186/1753-6561-7-S6-P17>
 12. Qian Y, Xing Z, Lee S, Mackin NA, He A, Kayne PS, He Q, Qian NX, Li ZJ (2014) Hypoxia influences protein transport and epigenetic repression of CHO cell cultures in shake flasks. *Biotechnol J* 9(11):1413–1424. <https://doi.org/10.1002/biot.201400315>
 13. Maschke RW, Seidel S, Bley T, Eibl R, Eibl D (2021) Determination of culture design spaces in shaken disposable cultivation systems for CHO suspension cell cultures. *Biochem Eng J* 177:108224. <https://doi.org/10.1016/j.bej.2021.108224>
 14. García-Ochoa F, Gomez E (2009) Bioreactor scale-up and oxygen transfer rate in microbial processes: an overview. *Biotechnol Adv* 27:153–176. <https://doi.org/10.1016/j.procbio.2007.08.001>
 15. Keane JT, Ryan D, Gray PP (2003) Effect of shear stress on expression of a recombinant protein by Chinese hamster ovary cells. *Biotechnol Bioeng* 81(2):211–220. <https://doi.org/10.1002/bit.10472>
 16. Godoy-Silva R, Mollet M, Chalmers JJ (2009) Evaluation of the effect of chronic hydrodynamical stresses on cultures of suspended CHO-6E6 cells. *Biotechnol Bioeng* 102(4):1119–1130. <https://doi.org/10.1002/bit.22146>
 17. Godoy-Silva R, Chalmers JJ, Casnocha SA, Bass LA, Ma N (2009) Physiological responses of CHO cells to repetitive hydrodynamic stress. *Biotechnol Bioeng* 103(6):1103–1117. <https://doi.org/10.1002/bit.22339>
 18. Ritacco FV, Wu Y, Khetan A (2018) Cell culture media for recombinant protein expression in Chinese hamster ovary (CHO) cells: history, key components, and optimization strategies. *Biotechnol Prog* 34(6):1407–1426. <https://doi.org/10.1002/btpr.2706>
 19. Zhang X, Bürki CA, Stettler M, De Sanctis D, Perrone M, Discacciati M, Parolini N, DeJesus M, Hacker DL, Quarteroni A, Wurm FM (2009) Efficient oxygen transfer by surface aeration in shaken cylindrical containers for mammalian cell cultivation at volumetric scales up to 1000 L. *Biochem Eng J* 45(1):41–47. <https://doi.org/10.1016/j.bej.2009.02.003>
 20. Nienow AW (2006) Reactor engineering in large scale animal cell culture. *Cytotechnology* 50:9–33. <https://doi.org/10.1007/s10616-006-9005-8>
 21. Büchs J, Maier U, Milbradt C, Zoels B (2000) Power consumption in shaking flasks on rotary shaking machines: II. Nondimensional description of specific power consumption and flow regimes in unbaffled flasks at elevated liquid viscosity. *Biotechnol Bioeng* 68(6):594–601. [https://doi.org/10.1002/\(SICI\)1097-0290\(20000620\)68:6%3c594::AID-BIT2%3e3.0.CO;2-U](https://doi.org/10.1002/(SICI)1097-0290(20000620)68:6%3c594::AID-BIT2%3e3.0.CO;2-U)
 22. Büchs J (2001) Introduction to advantages and problems of shaken cultures. *Biochem Eng J* 7(2):91–98. [https://doi.org/10.1016/S1369-703X\(00\)00106-6](https://doi.org/10.1016/S1369-703X(00)00106-6)
 23. Zhang H, Williams-Dalson W, Keshavarz-Moore E, Shamlou PA (2005) Computational-fluid-dynamics (CFD) analysis of mixing and gas-liquid mass transfer in shake flasks. *Biotechnol Appl Biochem* 41:1–8. <https://doi.org/10.1042/BA20040082>
 24. Tramper J, de Gooijer KD, Vlak JM (2020) Scale-up considerations and bioreactor development for animal cell cultivation. In: *Insect cell culture engineering*, 1er Ed. CRC Press. 139–177
 25. Pérez-Rodríguez SP, Wulff T, Voldborg BG, Altamirano C, Trujillo-Roldán MA, Valdez-Cruz NA (2021) Compartmentalized proteomic profiling outlines the crucial role of the classical secretory pathway during recombinant protein production in Chinese Hamster Ovary cells. *ACS Omega* 6(19):12439–12458. <https://doi.org/10.1021/acsomega.0c06030>
 26. Gonzalez TN, Leong SR, Presta LG (2000) Nucleic Acids Encoding Humanized Anti-IL-8 Monoclonal Antibodies. *US6025158A*
 27. Strober W (2015) Trypan blue exclusion test of cell viability. *Curr Protoc Immunol* 111(1):A3-B. <https://doi.org/10.1002/0471142735.ima03bs111>
 28. Reynoso-Cereceda GI, García-Cabrera RI, Valdez-Cruz NA, Trujillo-Roldán MA (2016) Shaken flasks by resonant acoustic mixing versus orbital mixing: mass transfer coefficient $k_L a$ characterization and *Escherichia coli* cultures comparison. *Biochem Eng J* 105(B):379–390. <https://doi.org/10.1016/j.bej.2015.10.015>
 29. Van'T Riet K (1979) Review of measuring methods and results in nonviscous gas-liquid mass transfer in stirred vessels. *Ind Eng Chem Process Des Dev* 18(3):357–364. <https://doi.org/10.1021/i260071a001>
 30. Büchs J, Maier U, Milbradt C, Zoels B (2000) Power consumption in shaking flasks on rotary shaking machines: I. Power consumption measurement in unbaffled flasks at low liquid viscosity. *Biotechnol Bioeng* 68(6):589–593. [https://doi.org/10.1002/\(SICI\)1097-0290\(20000620\)68:6%3c589::AID-BIT1%3e3.0.CO;2-J](https://doi.org/10.1002/(SICI)1097-0290(20000620)68:6%3c589::AID-BIT1%3e3.0.CO;2-J)
 31. García-Camacho F, Gallardo-Rodríguez J, Sánchez-Miron A, Cerón-Gracia M, Belarbi E, Molina-Grima E (2007) Determination of shear stress thresholds in toxic dinoflagellates cultured in shake flasks implications in bioprocess engineering. *Process Biochem* 42:1506–1515. <https://doi.org/10.1016/j.procbio.2007.08.001>
 32. Peter CP, Suzuki Y, Büchs J (2006) Hydromechanical stress in shake flasks: correlation for the maximum local energy dissipation rate. *Biotechnol Bioeng* 93(6):1164–1176. <https://doi.org/10.1002/bit.20827>
 33. Heinrich C, Wolf T, Kropp C, Northoff S, Noll T (2011) Growth characterization of CHO DP-12 cell lines with different high

- passage histories. *BMC Proc* 5(Suppl 8):P29. <https://doi.org/10.1186/1753-6561-5-S8-P29>
34. Sieck JB, Budach WE, Suemeghy Z, Leist C, Villiger TK, Morbidelli M, Soos M (2014) Adaptation for survival: phenotype and transcriptome response of CHO cells to elevated stress induced by agitation and sparging. *J Biotechnol* 189:94–103. <https://doi.org/10.1016/j.jbiotec.2014.08.042>
 35. Yoo HC, Yu YC, Sung Y, Han JM (2020) Glutamine reliance in cell metabolism. *Exp Mol Med* 52:1496–1516. <https://doi.org/10.1038/s12276-020-00504-8>
 36. Pörtner R (2009) Characteristics of mammalian cells and requirements for cultivation. In: Eibl R, Eibl D, Pörtner R, Catapano G, Czermak P (eds) *Cell and tissue reaction engineering*. Springer, Berlin, pp 13–53. https://doi.org/10.1007/978-3-540-68182-3_2
 37. Pörtner R (2015) Bioreactors for mammalian cells. In: Al-Rubeai M (ed) *Animal cell culture*. Springer, Dublin, pp 89–135. https://doi.org/10.1007/978-3-319-10320-4_4
 38. Bürgin T, Coronel J, Hagens G, Keebler MV, Genzel Y, Reich, U, Anderlei T (2020) Orbitally Shaken single-use bioreactor for animal cell cultivation: fed-batch and perfusion mode. In *Animal Cell Biotechnology* (pp. 105–123). Humana, New York, NY. https://doi.org/10.1007/978-1-0716-0191-4_7
 39. Kato Y, Tada Y, Iwanaga E, Nagatsu Y, Iwata S, Lee YS, Koh ST (2005) Effects of liquid film formed on flask surface on oxygen transfer rate in shaking flask and development of baffled shaking vessel by optical method based on sulfite oxidation. *J Chem Eng Jpn* 38(11):873–877. <https://doi.org/10.1252/jcej.38.873>
 40. Henzler HJ, Schedel M (1991) Suitability of the shaking flask for oxygen supply to microbiological cultures. *Bioprocess Eng* 7(3):123–131. <https://doi.org/10.1007/BF00369423>
 41. Giese H, Azizan A, Kümmel A, Liao A, Peter CP, Fonseca JA, Hermann R, Duarte TM, Büchs J (2014) Liquid films on shake flask walls explain increasing maximum oxygen transfer capacities with elevating viscosity. *Biotechnol Bioeng* 111(2):295–308. <https://doi.org/10.1002/bit.25015>
 42. Chopda VR, Holzberg T, Ge X, Folio B, Wong L, Tolosa M, Kostov Y, Tolosa L, Rao G (2020) Real-time dissolved carbon dioxide monitoring II: surface aeration intensification for efficient CO₂ removal in shake flasks and mini-bioreactors leads to superior growth and recombinant protein yields. *Biotechnol Bioeng* 117(4):992–998. <https://doi.org/10.1002/bit.272529981>
 43. Torres M, Zúñiga R, Gutierrez M, Vergara M, Collazo N, Reyes J, Berrios J, Aguillon JC, Molina MM, Altamirano C (2018) Mild hypothermia upregulates myc and xbp1s expression and improves anti-TNF α production in CHO cells. *PLoS ONE* 13(3):e0194510. <https://doi.org/10.1371/journal.pone.0194510>
 44. Toussaint C, Henry O, Durocher Y (2016) Metabolic engineering of CHO cells to alter lactate metabolism during fed-batch cultures. *J Biotechnol* 217:122–131. <https://doi.org/10.1016/j.jbiotec.2015.11.010>
 45. Konakovsky V, Clemens C, Müller MM, Bechmann J, Berger M, Schlatter S, Herwig C (2016) Metabolic control in mammalian fed-batch cell cultures for reduced lactic acid accumulation and improved process robustness. *Bioengineering (Basel)* 3(1):5. <https://doi.org/10.3390/bioengineering3010005>
 46. Sieck JB, Cordes T, Budach WE, Rhiel MH, Suemeghy Z, Leist C, Villiger TK, Morbidelli M, Soos M (2013) Development of a scaled-down model of hydrodynamic stress to study the performance of an industrial CHO cell line under simulated production scale bioreactor conditions. *J Biotechnol* 164:41–49. <https://doi.org/10.1016/j.jbiotec.2012.11.012>

Publisher's Note Springer Nature remains neutral with regard to jurisdictional claims in published maps and institutional affiliations.